Present-Day Volcanism on Venus: Evidence from Microwave Radiometry

N. V. Bondarenko,[1,2] J. W. Head,[3] and M. A. Ivanov[3,4]

Received 23 August 2010; revised 28 September 2010; accepted 5 October 2010; published 8 December 2010.

[1] We present new evidence for volcanic eruptions and lava flow emplacement on Venus within the last several decades. An integrated study of a radar-dark lava flow unit in Bereghinia Planitia on Venus (~28°E, ~39°N) based on Magellan data obtained in 1993 reveals a significant apparent microwave thermal emission excess, consistent with increased subsurface temperature due to very recent lava flow emplacement. The flow unit occupies the stratigraphically youngest position in the area and in part is more than 15 years old because it was also observed in the radar map obtained by Pioneer-Venus in 1978. Analysis of lava flow cooling rates and geological characteristics point to flow material of mafic composition. Future missions can employ this microwave radiometry technique to search for and monitor active volcanism on Venus. **Citation:** Bondarenko, N. V., J. W. Head, and M. A. Ivanov (2010), Present-Day Volcanism on Venus: Evidence from Microwave Radiometry, *Geophys. Res. Lett.*, *37*, L23202, doi:10.1029/2010GL045233.

1. Introduction

[2] To date there have been no direct observations of volcanic eruptions on Venus. On the basis of its geologically young surface, current volcanic activity is expected, but still unproven. On Earth, which is similar to Venus in size, eruptive activity has been constantly recorded during the last century. For example, the Hawaii Islands are known for the eruptions of Mauna Iki (1919–1920), Mauna Ulu (1969–1974), and Pu'u 'O'o-Kupaianaha (1983-ongoing), each accompanied by dozens of dike emplacement events and eruptions producing lava flows [*Wilson and Head*, 1988; *Rowland and Munro*, 1993; *Peterson et al.*, 1994; *Heliker*, 2002].

[3] Several types of observations have been cited as indirect evidence of historically recent volcanism on Venus. A rapid decrease of SO_2 abundance at the cloud tops of Venus during an eight-year period recorded by Pioneer Venus has been interpreted to be due to injection of a large quantity of SO_2 caused by a volcanic eruption a few years before these observations [*Esposito et al.*, 1988]. Ongoing volcanism on Venus has also been hypothesized based on lightning discharges [*Russell et al.*, 2007].

[4] Recent Venus Express VIRTIS (Visible and Infrared Thermal Imaging Spectrometer) observations have shown strong near-IR emissivity anomalies associated with the stratigraphically youngest flows in Imdr, Themis, and Dione Regiones [*Smrekar et al.*, 2010], each of which had been identified earlier as candidate hot spots on the basis of geologic mapping. In a manner similar to Hawaii on Earth, hot spots on Venus have volcanic edifices, broad topographic swells, and large positive gravity anomalies [e.g., *Phillips and Malin*, 1984]. VIRTIS emissivity anomalies have been interpreted as flow material much fresher and less weathered than subjacent material. These flows were estimated to be as young as 250,000 years or less [*Smrekar et al.*, 2010].

[5] In the present analysis we use a different approach and discuss evidence for very recent volcanism in the Venus lowlands. The approach proposed here allows us to search for recent lavas with microwave radiometry through the detection of enhanced flow temperatures at shallow depths below the flow surface.

2. Thermal State of Fresh Lava Flows on Venus

[6] In general, cooling of hot lavas is controlled by natural and forced convection in the atmosphere, radiation from all exposed lava surfaces, and conductive heat transfer into the underlying ground. The surface of a lava flow in a lowland area on Venus will be cooled down to 900 K in ~43 minutes, and to 780 K in ~2 days after emplacement [*Head and Wilson*, 1986]. Taking account of absorption of radiation by CO_2 in the near-surface atmosphere layer can prolong these durations by ~40% [*Snyder*, 2002]. A lava flow that is already cool at the surface (and hence indistinguishable as hot in visible and infrared observations) will remain hot in the deeper subsurface. For example, on Earth in a rather thick (>45 m) lava flow the basaltic lava solidus temperature of 1475 K is still expected to be encountered at depths of ~7 m after ~1.3 years and ~23 m after ~12 years following the eruption (recalculated from *Head and Wilson* [1986] based on a lava thermal conductivity of 1.5 W m^{-1} K^{-1} [*Vosteen and Schellschmidt*, 2003]). On Venus, solidus depths for similar time intervals are predicted to be shallower with higher solidus temperatures (1525 K) [*Head and Wilson*, 1986], resulting in an ~800 K temperature excess over atmospheric temperature.

[7] We calculated temperature changes in a lava flow and the underlying substrate as a function of time by solving the 1D heat diffusion equation, with boundary conditions prescribing the temperature at the flow surface and at infinite depth under the surface to be equal to 741 K (the temperature of the reference Venus atmosphere at an altitude of 6051 km). Figure 1 shows the depth dependence of the subsurface temperature excess over atmospheric temperature for a 15 years

[1]Earth and Planetary Sciences, University of California, Santa Cruz, California, USA.
[2]Usikov Institute of Radiophysics and Electronics, National Academy of Science of Ukraine, Kharkov, Ukraine.
[3]Department of Geological Sciences, Brown University, Providence, Rhode Island, USA.
[4]Vernadsky Institute, Russian Academy of Sciences, Moscow, Russia.

0094-8276/10/2010GL045233

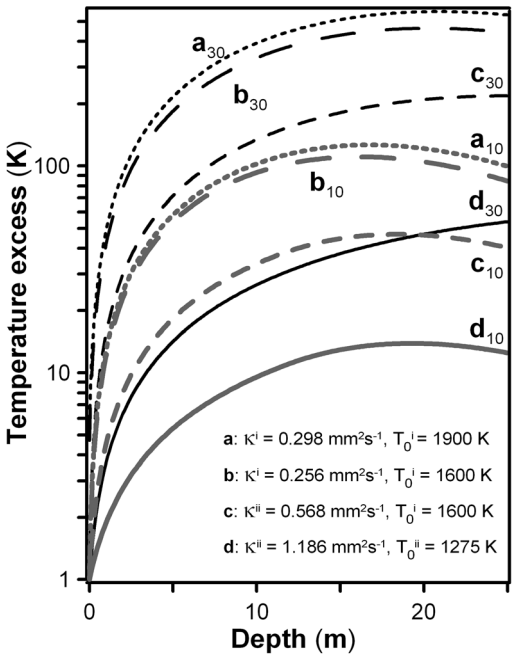

Figure 1. Temperature excess over near-surface atmosphere temperature versus depth for a 15 year old lava flow having ultramafic (a), mafic (b, c), and felsic (d) composition. Subscripts denote flow thicknesses of 10 m and 30 m; superscripts indicate values from (i) *Davies et al.* [2005] and (ii) *Petcovic and Dufek* [2005].

old lava flow with thicknesses of 10 m and 30 m, and different lava compositions corresponding to different initial temperatures T_0 and different thermal diffusivities κ. Calculations (Figure 1) were made considering a mafic composition for the substrate ($\kappa = 0.238$ mm^2 s^{-1} [*Davies et al.*, 2005]), and lavas having ultramafic (komatiite), mafic (basalt), and felsic (tonalite) compositions (particular values of κ and T_0 are shown in Figure 1; κ was derived using data from *Davies et al.* [2005] and *Petcovic and Dufek* [2005]). Figure 1 shows that a thicker flow, lower κ and higher T_0 help to maintain a high subsurface temperature for a longer time. Significantly increased temperatures are expected for a 30 m thick flow for decades.

3. Apparent Radio Brightness Temperature of a Fresh Lava Flow

[8] The radio brightness temperature T_B just above the flow surface observed by a radiometer at an angle θ to the nadir is related to the apparent flow temperature T_{AP} [*Ulaby et al.*, 1986] by

$$T_B(\theta) = e(\theta)\, T_{AP}(\theta'), \quad e(\theta) = 1 - \Gamma^*(\theta), \tag{1}$$

where θ' is the incidence angle of radiation inside the flow (in the case of a smooth boundary, θ' is related to θ through Snell's law, e.g., [*Stratton*, 1947]), and $e(\theta)$ is the flow emissivity. According to Kirchoff's law, the latter is expressed through Γ^*, the total reflectivity describing radiation scattered into the upper hemisphere if the surface is illuminated at the angle θ.

[9] In the case of homogeneous flow media with a non-uniform temperature profile $T(z)$, an apparent temperature of the flow T_{AP} is expressed as [*Ulaby et al.*, 1986]

$$T_{AP}(\theta') = \sec\theta' \int_0^\infty \kappa_a T(z) \exp(-\sec\theta'\ \tau(z))dz, \quad \tau(z) = \int_0^z \kappa_a dz \tag{2}$$

Here $\tau(z)$ is the optical thickness down to depth z and κ_a is the flow media absorption coefficient. For nonmagnetic homogeneous media, κ_a is approximately proportional to tan $\delta\ \varepsilon^{0.5}\ \lambda^{-1}$, where ε and tan δ are the media dielectric permittivity and loss factor, respectively, and λ is the wavelength of observation.

[10] In the state of thermal equilibrium ($T(z)$ = constant), T_{AP} is the physical temperature of the flow. With homogeneous flow material, a uniform temperature profile and a smooth upper flow interface, 80% of the total thermal emission is formed in the upper layer from the surface down to $\tau = 1.7$, 90% – to $\tau \approx 2.4$, and 100% – to $\tau \approx 10$. For example, considering observations at $\lambda = 12.6$ cm and flow material having $\varepsilon = 6.48$ and tan $\delta = 0.004$, 10% of the total thermal emission is formed at depths of 5 to 21 m. This estimate shows that a noticeable part of the thermal emission probes the rather deep subsurface. If the flow subsurface is warmer, the relative contribution of deep layers is even higher. If the wavelength of observation λ is 31 cm, 10% of the total thermal emission comes from depths of 11.6 to 49.1 m. In contrast, a λ of 3.5 cm is able to sense the subsurface only to depths of ~3 m.

[11] If the flow is warmer than the underlying surface, the apparent flow temperature excess over the near-surface atmosphere temperature is shown in Figure 2 as a function of the flow material's loss factor, tan δ. The flow is assumed to be

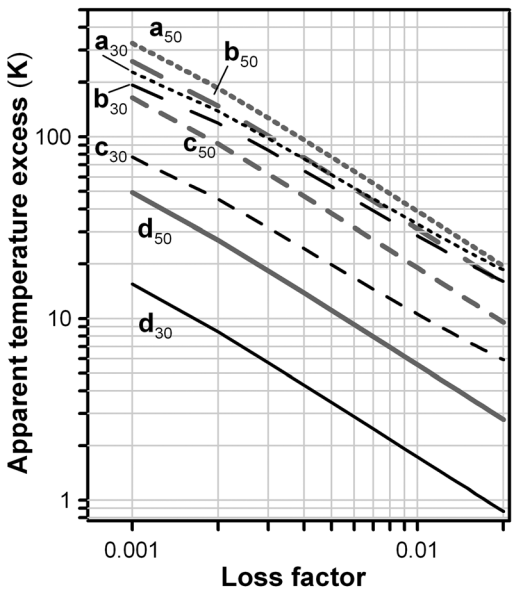

Figure 2. The apparent flow temperature excess over the near-surface atmosphere as a function of flow material loss factor for a 15 years old lava flow having ultramafic (a), mafic (b, c), and felsic (d) compositions with $\varepsilon = 6.48$. Subscripts denote flow thickness of 30 m and 50 m. Thermal parameters are the same as in Figure 1.

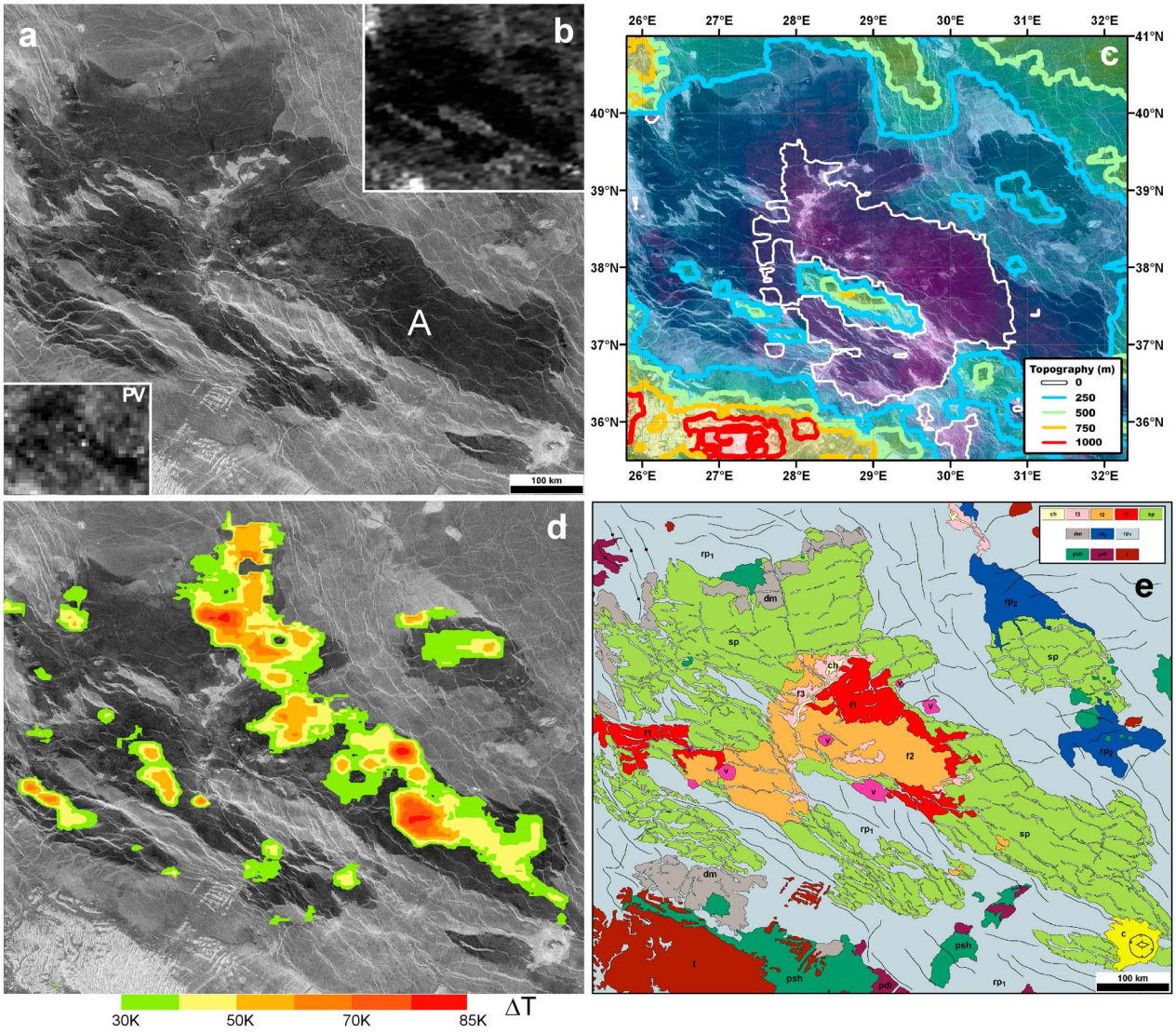

Figure 3. Radar dark flow in Bereghinia Planitia: (a) Magellan SAR image; (b) large-scale roughness map (from GxDR data set); (c) Magellan altimetry data in topographic map form, overlain on Magellan SAR image; contour interval is 250 m, with white contour lowest and red contour highest; (d) calculated ΔT overlain on Magellan image shown in Figure 3a; (e) geological map. Legend: v, volcano; ch, channel; f1, f2, f3, lava flow units; sp, smooth plain; dm, dark marginal material; rp1, rp2, rough regional plains; psh, shield plains; pdl, densely lineated plains; t, tessera; c, crater. PV inset is Pioneer-Venus radar image of the flow (1978).

15 years old, 30 m or 50 m thick, homogeneous, to have ε = 6.48, and the same compositions as in Figure 1. Figure 2 shows that smaller tan δ allows sensing to deeper subsurface levels.

[12] If the flow is still not cooled down, the T_{AP} of the flow has to be higher in comparison with the value expected from the near-flow atmosphere temperature. When radiometric measurements are used for the extraction of surface emissivity under the assumption of the thermal equilibrium state (equation (1)), an enhanced T_{AP} leads to overestimation of emissivity. We now apply these concepts to Venus.

4. A Candidate Fresh Lava Flow in Bereghinia Planitia

[13] We undertook a global survey of regions with unusual microwave properties. Among a number of interesting areas, we found a lava flow unit with rather unique microwave properties, located at about 28°E, 39°N in Bereghinia Planitia. The flow unit (Figure 3a) is radar dark as seen in the Magellan SAR image (at an incidence angle θ of ~39°), and in Earth-based observations at θ = ~60° [*Carter et al.*, 2004]. Thus the flow is smooth at spatial scales of centimeters, a scale that controls oblique backscattering.

[14] The flow is also very smooth at decameter spatial scales in the Magellan roughness map (average roughness is ~0.7°) [*Ford and Pettengill*, 1992] (Figure 3b). The linear polarization coefficients map published by *Carter et al.* [2004] shows that this flow exhibits up to 12% linear polarization when illuminated by a circularly polarized signal. This can occur only when the target surface is very smooth and rather transparent to radio waves, so that the waves scattered at internal interfaces or inclusions can reach the

observer. The radar dark flow unit occurs in three strips, all oriented parallel to the NW-SE-trending grain of the regional topography (Figure 3c) and to the NW-SE-trending set of regional wrinkle ridges. The northeast strip is the largest of the three, about 900 km long and 100–200 km wide.

[15] The T_{AP} over the flow unit was calculated from the observed radio brightness temperature (resolution 34 × 25 km, accuracy σ_T = ~15 K) [*Pettengill et al.*, 1992] following equation (1) and assuming a smooth upper flow interface. In this case Γ* can be calculated using the Fresnel equations. Magellan observations allow estimates of surface dielectric permittivity ε through "Fresnel reflectivity" R_0 derived from the Magellan altimeter experiment [*Ford and Pettengill*, 1992] (resolution 16 km × 8 km, accuracy σ_{R0} ~ 30%). The Hagfors function used there for reflectivity estimates is stated as the best fit scattering law for the area [*Tyler et al.*, 1992]. (Since reflectivity estimate is model dependent, the use of another scattering function can give other values of surface dielectric permittivity and, therefore, can shift the final results of the calculations.) Since the lava flow has a smooth upper interface (which excludes emissivity enhancement due to roughness), a positive excess of the apparent temperature ΔT over the physical temperature of the surface is most likely to be due to increased subsurface temperature.

[16] The ΔT calculated over the flow (Figure 3d) varies from an equilibrium state (no thermal excess), up to ~85 K. Eleven percent of the entire flow surface shows ΔT higher than $3\sigma_T$. A continuous NW-SE alignment of high ΔT values characterizes the northeastern strip of radar-dark plains. Some of the highest ΔT values are associated with the radar darkest flow segments (e.g., site *A* in Figure 3a). Low (or no) thermal excess is usually seen in the marginal areas of the radar dark region (Figure 3d). The topographic map (Figure 3c) shows that the linear concentration of highest ΔT values (Figure 3d) is associated with the topographically lowest parts of the northeastern radar dark strip. The flow area exhibits a median "DELTA"T of ~36 K which is much higher than the value of ~3 K characterizing the "cold" dark halo of the 10 km crater Zosia (18.9"deg"S, 109.2"deg"E) which has a decameter-scale roughness and dark apperance in radar images similar to the area under study.

[17] We used high-resolution Magellan SAR mosaics (F-maps) and standard cross-cutting, embayment, and superposition relationships (e.g., [*Ivanov*, 2008]) to compile a geological map of the region (Figure 3e) and assess the relative ages of the units. These relationships clearly show that the radar-dark flow unit (Figure 3a) is younger in comparison with the surrounding brighter surface. The dark material clearly embays large arches and smaller wrinkle ridges, truncates narrow radar-bright lineaments, and is emplaced along the older NW-SE regional topographic troughs formed by the undulating surface of older units (compare Figures 3a, 3c, and 3e).

[18] Older geologic units (t, pdf and psh) are exposed along a major ridge in the southwest and have been embayed by unit dm and regional volcanic plains units rp_1 and rp_2; rp_1 and rp_2 were then deformed into broad NW-SE trending arches and troughs (Figure 3c), and by pervasive NW-SE-trending wrinkle ridges. The radar dark flow unit is superposed on these older broadly deformed regional plains units (rp_1, rp_2) and fills troughs between the broad arches (Figure 3c). The radar dark flow unit can be divided into five subunits: a broad smooth plains unit (sp), individual flow units 1, 2, 3 (f1, f2, f3), and a channel unit (ch). The narrow channels, lobate flow fronts and several flow units provide evidence for multiple stages in the eruptions, similar to those on Earth. The shapes and sizes of flow lobes and units, the surface smoothness, and the ponding and filling of topographic lows, point to a mafic composition of the flow material [*Head et al.*, 1992; *Guest et al.*, 1992]. We interpret these units to represent a lava flow complex consisting of multiple flow units: these include proximal vents, channels and slightly rougher (radar brighter) marginal and levee deposits (units v, ch, f3), intermediate flow lobes (units f1 and f2) and distal, very smooth, ponded flow deposits (unit sp).

[19] At least parts of the broad flow unit under study have to be older than 15 years before the Magellan images were obtained (Figure 3) because the broad feature is recognizable in the radar map obtained during the Pioneer-Venus mission in 1978 (see PV inset to Figure 3a). To provide a ΔT similar to the one calculated for a 15 years old, 30 m thick flow (Figure 3d), lava needs to have mafic or ultramafic composition and low losses, tan $\delta < 0.005$ (Figure 2). Ultramafic peridotite rock (sampled at Lowell, Vt.) exhibits a tan δ of 0.008 and ε = 7.5 [*Campbell and Ulrichs*, 1969]. Although basalts usually have higher losses, such low tan δ values for materials of basaltic composition are known for returned lunar samples with low $FeO+TiO_2$. A tan δ of 0.004 corresponds to 7.92% of $FeO+TiO_2$ oxides as calculated using the formula for lunar rock samples of *Carrier et al.* [1991]. This value is close to the abundances of $FeO+TiO_2$ measured *in situ* by Venera – 13 (10.9%, upland rolling plains), Venera – 14 (9.9%, flat lowlands), and by Vega – 2 (7.9%, the northern slope of the high-mountain massif Aphrodite Terra), interpreted to have a composition close to alkaline and thoeliitic basalts, and olivine gabbro-norite, respectively [*Barsukov*, 1992]. Additionally, lunar crystalline melt breccias 62235 (ε = 6.52, tan δ = 0.0066), 14310 (ε = 6.58, tan δ = 0.0044), and 65015 (ε = 7, tan δ = 0.008) show $FeO+TiO_2$ contents of 10.65%, 9%, and 9.85%, respectively [*Carrier et al.*, 1991]. Apollo 15 low Ti pigeonite basalt 15597 has ε = 6.16, tan δ = 0.002, and 20% FeO [*Carrier et al.*, 1991].

[20] Variations in ΔT over the flow (Figure 3d) can be partly explained by variations of flow thickness, for example, thinner flows in areas closer to the flow margins. The "sp" unit (Figure 3e) partly covers large wrinkle ridges. The heights of such wrinkle ridges were estimated to be ~40 to 90 m [*Connors*, 1995] and ~50 to 260 m [*Kreslavsky and Basilevsky*, 1998]. Thus it is reasonable to expect the flow under study to be at least as thick as 30 to 50 m in some locations, and perhaps even more.

[21] The highest ΔT is ~85 K in the "sp" unit and ~60 K in the "f1", "f2" and "f3" units (Figures 3d and 3e). In single lava flow emplacement phases, multiple overlapping flow lobes and subunits often occur. Scattering at subsurface interfaces of these rather thin sublayers that are transparent to radio waves can explain this ΔT difference due to an overestimated flow emissivity as discussed by *Bondarenko* [2010]; this can cause an underestimation of apparent flow temperature. Low values of ΔT in the marginal areas are likely to be due to thinner and more rapidly cooled flow margins or to flows emplaced somewhat earlier in the flow sequence.

[22] The average value of ε calculated over the northeast strip of the flow is equal to 4.26. In general, ε varies over the

range of 3.01–6.48 in the flow area. The highest ε is observed in site *A* (Figure 3a) and corresponds to the darkest flow part in the SAR image; here the density of wrinkle ridges is also lower.

5. Conclusions

[23] The radar properties of the radar-dark smooth plains flow unit in Bereghinia Planitia are consistent with a presently-existing temperature excess at shallow depth within the unit. This implies very recent lava flow emplacement, within the last several decades. The theoretical rate of lava cooling, the apparent brightness temperature of the plains, and their geological relationships with the surrounding units collectively suggest that the plains have a mafic composition characterized by low microwave losses. Variations of ΔT over the flow can be explained by variations of flow thickness and are consistent with the emplacements of lava channels, flows and broad flow units. The combination of microwave radiometry and scatterometry is recommended as a technique for future missions for the detection, monitoring and the study of ongoing lava emplacement on the surface of Venus.

[24] **Acknowledgments.** Authors gratefully acknowledge L. Wilson and an anonymous reviewer for their positive and useful comments which improved the paper. The authors also appreciate the very helpful in depth discussions with P. Ford in reflectivity estimates.

References

Barsukov, V. L. (1992), Venusian igneous rocks, in *Venus Geology, Geochemistry, and Geophysics: Research Results From the USSR*, edited by V. L. Barsukov et al., pp. 165–176, Univ. of Ariz. Press, Tucson.

Bondarenko, N. V. (2010), Integrated study of the Venus surface with Magellan data: An opportunity to search for surficial deposits and warm lava flows, *Lunar Planet. Sci.*, *XLI*, Abstract 1579.

Campbell, M. J., and J. Ulrichs (1969), Electrical properties of rocks and their significance for lunar radar observations, *J. Geophys. Res.*, *74*, 5867–5881, doi:10.1029/JB074i025p05867.

Carrier, W. D., III, G. R. Olhoeft, and W. Mendell (1991), Physical properties of the lunar surface, in *Lunar Source-Book: A User's Guide to the Moon*, edited by G. H. Heiken, D. T. Vaniman, and B. M. French, pp. 530–552, Cambridge Univ. Press, New York.

Carter, L. M., D. B. Campbell, and B. A. Campbell (2004), Impact crater related surficial deposits on Venus: Multipolarization radar observations with Arecibo, *J. Geophys. Res.*, *109*, E06009, doi:10.1029/2003JE002227.

Connors, C. (1995), Determining heights and slopes of fault scarps and other surfaces on Venus using Magellan stereo radar, *J. Geophys. Res.*, *100*, 14,361–14,381, doi:10.1029/95JE01134.

Davies, A. G., D. L. Matson, G. J. Veeder, T. V. Johnson, and D. L. Blaney (2005), Post-solidification cooling and the age of Io's lava flows, *Icarus*, *176*, 123–137, doi:10.1016/j.icarus.2005.01.015.

Esposito, L. W., M. Copley, R. Eckert, L. Gates, A. I. F. Stewart, and H. Worden (1988), Sulfur dioxide at the Venus cloud tops, 1978–1986, *J. Geophys. Res.*, *93*, 5267–5276, doi:10.1029/JD093iD05p05267.

Ford, P. G., and G. H. Pettengill (1992), Venus topography and kilometer-scale slopes, *J. Geophys. Res.*, *97*, 13,103–13,115, doi:10.1029/92JE01085.

Guest, J., M. Bulmer, J. Aubele, K. Beratan, R. Greeley, J. Head, G. Michaels, C. Weitz, and C. Wiles (1992), Small volcanic edifices and volcanism in the plains of Venus, *J. Geophys. Res.*, *97*, 15,949–15,966, doi:10.1029/92JE01438.

Head, J. W., and L. Wilson (1986), Volcanic processes and landforms on Venus: Theory, predictions, and observations, *J. Geophys. Res.*, *91*, 9407–9446, doi:10.1029/JB091iB09p09407.

Head, J. W., L. Crumpler, J. Aubele, J. Guest, and R. S. Saunders (1992), Venus volcanism: Classification of volcanic features and structures, associations, and global distribution from Magellan data, *J. Geophys. Res.*, *97*, 13,153–13,197, doi:10.1029/92JE01273.

Heliker, C. (2002), The Pu'u 'O'o-Kupaianaha eruption of Kilauea Volcano: The first 20 years, *Eos Tans. AGU*, *83*(47), Fall Meet. Suppl., Abstract V62C-01.

Ivanov, M. (2008), Global geologic map of Venus: Preliminary results, *Lunar Planet. Sci.*, *XXXIX*, Abstract 1017.

Kreslavsky, M. A., and A. T. Basilevsky (1998), Morphometry of wrinkle ridges on Venus: Comparison with other planets, *J. Geophys. Res.*, *103*, 11,103–11,111, doi:10.1029/98JE00360.

Petcovic, H. L., and J. D. Dufek (2005), Modeling magma flow and cooling in dikes: Implications for emplacement of Columbia River flood basalts, *J. Geophys. Res.*, *110*, B10201, doi:10.1029/2004JB003432.

Peterson, D. W., R. T. Holcomb, R. I. Tilling, and R. L. Christiansen (1994), Development of lava tubes in the light of observations at Mauna Ulu, Kilauea Volcano, Hawaii, *Bull. Volcanol.*, *56*, 343–360, doi:10.1007/s004450050044.

Pettengill, G. H., P. G. Ford, and R. J. Wilt (1992), Venus surface radiothermal emission as observed by Magellan, *J. Geophys. Res.*, *97*, 13,091–13,102, doi:10.1029/92JE01356.

Phillips, R. J., and M. C. Malin (1984), Tectonics of Venus, *Annu. Rev. Earth Planet. Sci.*, *12*, 411–443, doi:10.1146/annurev.ea.12.050184.002211.

Rowland, S. K., and D. C. Munro (1993), The 1919–1920 eruption of Mauna Iki, Kilauea: Chronology, geologic mapping, and magma transport mechanisms, *Bull. Volcanol.*, *55*, 190–203, doi:10.1007/BF00301516.

Russell, C. T., L. Zhang, M. Delva, W. Magnes, R. J. Strangeway, and H. Y. Wei (2007), Lightning on Venus inferred from whistler-mode waves in the ionosphere, *Nature*, *450*, 661–662, doi:10.1038/nature05930.

Smrekar, S. E., E. R. Stofan, N. Mueller, A. Treiman, L. Elkins-Tanton, J. Helbert, G. Piccioni, and P. Drossart (2010), Recent hotspot volcanism on Venus from VIRTIS emissivity data, *Science*, *328*, 605–608, doi:10.1126/science.1186785.

Snyder, D. (2002), Cooling of lava flows on Venus: The coupling of radiative and convective heat transfer, *J. Geophys. Res.*, *107*(E10), 5080, doi:10.1029/2001JE001501.

Stratton, J. A. (1947), *Electromagnetic Theory*, 615 pp., John Wiley, New York.

Tyler, G. L., R. A. Simpson, M. J. Maurer, and E. Holmann (1992), Scattering properties of the venusian surface: Preliminary results from Magellan, *J. Geophys. Res.*, *97*, 13,115–13,139, doi:10.1029/92JE00742.

Ulaby, F. T., R. K. Moore, and A. K. Fung (1986), *Microwave Remote Sensing: Active and Passive*, Artech House, Norwell, Mass.

Wilson, L., and J. W. Head (1988), Nature of local magma storage zones and geometry of conduit systems below basaltic eruption sites: Pu'u O'o, Kilauea, East Rift, Hawaii example, *J. Geophys. Res.*, *93*, 14,785–14,792, doi:10.1029/JB093iB12p14785.

Vosteen, H.-D., and R. Schellschmidt (2003), Influence of temperature on thermal conductivity, thermal capacity and thermal diffusivity for different types of rock, *Phys. Chem. Earth*, *28*, 499–509, doi:10.1016/S1474-7065(03)00069-X.

N. V. Bondarenko, Earth and Planetary Sciences, University of California, 1156 High St., Santa Cruz, CA 95064, USA. (nbondar@ucsc.edu)

J. W. Head and M. A. Ivanov, Department of Geological Sciences, Brown University, Box 1846, Providence, RI 02912, USA.